PHYSICAL REVIEW C **67**, 041603(R) (2003)

$T=5/2$ states in ^{9}Li: Isobaric analog states of ^{9}He

G. V. Rogachev,[1] V. Z. Goldberg,[1,2,3] J. J. Kolata,[1] G. Chubarian,[3,4] D. Aleksandrov,[2] A. Fomichev,[4] M. S. Golovkov,[4] Yu. Ts. Oganessian,[4] A. Rodin,[4] B. Skorodumov,[1,2] R. S. Slepnev,[4] G. Ter-Akopian,[4] W. H. Trzaska,[5] and R. Wolski[4,6]

[1]*Physics Department, University of Notre Dame, Notre Dame, Indiana 46556*

[2]*Russian Research Centre "Kurchatov Institute," Moscow, Russia*

[3]*Texas A&M University, College Station, Texas 77843*

[4]*Joint Institute of Nuclear Research, Dubna, Russia*

[5]*Physics Department, University of Jyväskylä, Jyväskylä, Finland*

[6]*Institute of Nuclear Physics, Krakow, Poland*

(Received 5 February 2003; published 25 April 2003)

The thick target inverse kinematic method was applied to the study of isobaric analog states in the neutron-rich nucleus ^{9}Li. For this purpose, an excitation function for ^{8}He$+p$ elastic scattering was measured in the center-of-momentum energy range from 1.6 to 5.8 MeV. Three $T=5/2$ states in ^{9}Li (isobaric analogs of ^{9}He) were observed. Restrictions on the spin-parity assignments are provided according to *R*-matrix calculations, and conclusions regarding the structure of ^{9}He are given.

DOI: 10.1103/PhysRevC.67.041603 PACS number(s): 25.60.Bx, 21.10.Hw, 27.20.+n

Examining nuclear matter under extreme conditions makes the most demanding test of models of nuclear structure. An opportunity is provided by the study of nuclei far removed from the valley of stability. In particular, the ^{9}He nucleus gives an example of nuclear structure beyond the neutron drip line, i.e., ^{9}He has no states that are bound with respect to neutron emission. Since the time of its first observation [1], a $(1/2^{-})$ state, unstable by 1.2 MeV to neutron decay, was considered to be the ground state of ^{9}He. The authors of Ref. [1] compared positions of the observed levels with theoretical predictions of Ref. [2] and noted that these predictions, based on calculations for nuclei on the stability line, appear to be remarkably good for ^{9}He [1]. It is difficult to reach the ^{9}He nucleus, which is well beyond the region of nuclear stability, using conventional beams of stable nuclei. A group in the Hahn-Meitner Institute [3,4] developed a technique to obtain high resolution spectra of the products of complicated, low cross section binary (or quasibinary) reactions induced by conventional heavy ions. In this way, they managed to identify groups in the spectrum of the complementary product of the reactions as states in ^{9}He. Also, in spite of the inclusive character of the spectra and the low counting statistics they managed to estimate the widths of several states in ^{9}He. As for the spin parity determination, the complicated character of the process did not give a possibility for the direct determination of quantum characteristics of the levels. Still, some tentative assignments of spins were made on the basis of current theoretical predictions for the ^{9}He spectrum [3–5]. No contradictions with the calculations were observed.

Recently [6] the low-energy spectrum of ^{9}He produced in a direct reaction induced by a radioactive beam was studied via the final state interaction of ^{8}He$+n$. It was found [6] that an $s(1/2^{+})$ state was the ^{9}He ground state; the energy above the threshold for ^{8}He$+n$ decay was less than 0.2 MeV. After this result was reported, calculations [7] appeared that gave the $1/2^{+}$ state as the ground state of ^{9}He. However, the specific value of the binding energy of the virtual level [6] seems to be too large to agree with the instability of ^{10}He [8].

It seems rather clear that one needs a method for spin-parity determination of the states of dripline nuclei to obtain information that is independent of theoretical predictions in order to specify possible new features of unusual nuclei.

It is known [9–12] that the thick target inverse kinematics (TTIK) method can be used to study resonance reactions induced by radioactive beams. Recently, the study of isobaric analog states of neutron rich nuclei by this method has been proposed [13]. The spectroscopy of $T=5/2$ levels in ^{9}Li, which can be populated by means of ^{8}He$+p$ scattering, is directly related to the data on ^{9}He states. Even if the latter were complete, a detailed joint analysis of the data on $T=5/2$ states in ^{9}Li and in ^{9}He could give important information on the Coulomb interaction in these neutron-rich nuclei. This work presents the first results of a study of the $T=5/2$ states in ^{9}Li (isobaric analogs of the ^{9}He states) by the TTIK method. No $T=5/2$ states in ^{9}Li were previously known.

The experiment was performed with radioactive beams of ^{8}He at laboratory energy of 51 and 59 MeV having an intensity of about 1000/s, produced in the Flerov Laboratory (Dubna). The experimental setup is shown in Fig. 1. A primary beam of 32 MeV/A ^{11}B ions was incident on a very thick beryllium target. The spectrometer ACCULINNA [14] was used to separate ^{8}He from all other reaction products. The beam was then slowed by a thick Be wedge. Two thin plastic detectors in the flight path, upstream of the experi-

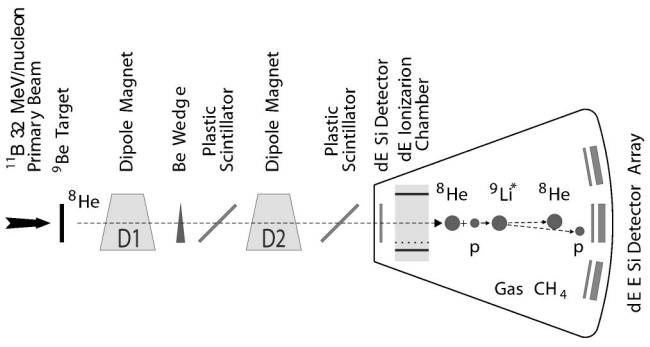

FIG. 1. Experimental setup. See text for description.

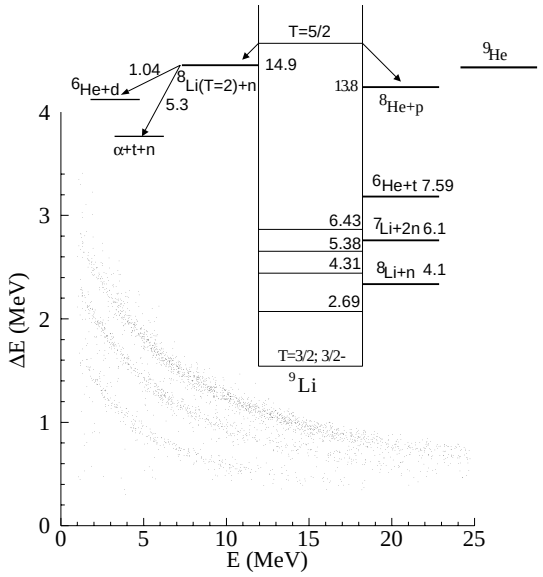

FIG. 2. Zero degree ΔE-E telescope spectrum for the products of the reaction of ^{8}He with the methane gas. Proton, deuteron, and triton bands are shown.

mental area, provided an event-by-event identification of the incoming particles. The scattering of ^{8}He on p was performed in a 50-cm scattering chamber filled with methane gas. The gas pressure was adjusted to stop the ^{8}He beam in front of a ΔE-E telescope positioned at 0° to the beam. The gas volume was separated from the vacuum by a 38-μm organic foil ($H_{31}C_{50}N_7O_7Cl_6$). A 60-μm Si detector was positioned at the entrance to the scattering chamber. A short (80 mm) windowless ionization chamber was inserted after the Si detector. The working gas of the ionization chamber was the methane gas of the scattering chamber. These detectors provided the final identification of the ^{8}He ions and discriminated against events occurring in the Si detector or the window foil. Three ΔE-E telescopes, one at 0° and one on each side of the central telescope, identified the products of the reactions of ^{8}He with the target gas. In addition, the time of flight between the plastic detector and the ΔE detector of each telescope was measured with a resolution of about 1 ns. This setup reduced the rate of random coincidences to a negligible level. A comparison of spectra obtained at different angles gave a check for the absence of any evident contribution from beam contaminant particles in the 0° detectors after offline selection.

Figure 2 gives the ΔE-E 0° spectrum for the products of the reactions of ^{8}He with methane gas. The interactions of ^{8}He with carbon and hydrogen can contribute to this spectrum. Measurements with CO_2 as the target gas showed that the carbon contribution to the spectrum in Fig. 2 is negligible. This finding agrees with the basis on which the TTIK method has been developed: the dominant process is elastic resonance scattering. One does not expect resonances in the ^{8}He+C interaction. However, it is clearly seen in Fig. 2 that the intensity of the proton spectrum does not dominate, unlike in previous applications of the method to the study of resonances in proton-rich nuclei [9–12].

In the ^{8}He+p resonance interaction, the excitations of ^{9}Li levels with $T=3/2$ or $T=5/2$ are allowed in accordance with isobaric spin conservation. Strong resonance population of unknown $T=3/2$ resonances is not expected due to the small ratio of the proton width of the initial channel to the total width of the hypothetical $T=3/2$ resonances. There are at least 16 modes of decay of the $T=3/2$ levels, and these modes are characterized by a more favorable penetrability than the ^{8}He+p channel.

Only two decay channels are allowed by T conservation for the lowest states with $T=5/2$ (see inset in Fig. 2). These are the initial channel ^{8}He+p, and its isobaric conjugate, ^{8}Li($T=2$)+n. The wave functions of $T=5/2$ states can be expressed through the single particle configurations in question as follows [15]:

$$\Psi_{^9\mathrm{Li}(T=5/2)} = \frac{1}{\sqrt{5}}\Psi_{^8\mathrm{He}+p} + \frac{2}{\sqrt{5}}\Psi_{^8\mathrm{Li}(T=2)+n}. \qquad (1)$$

The spin Clebsch-Gordan coefficients are omitted in Eq. (1) because the spin of the core is zero. We will use Eq. (1) to estimate partial widths for the p and n decay of the $T=5/2$ states, and also to evaluate the positions of $T=5/2$ analog resonances in ^{9}Li.

It follows from Eq. (1) that neutron decay of the $T=5/2$ states is four times more probable than proton decay. The neutron decay of the $T=5/2$ states will populate the lowest $T=2$ excited state in ^{8}Li (see inset in Fig. 2). This state, the isobaric analog of the ^{8}He ground state, can undergo only T-violating decays. The details of the decay of this $T=2$ state are still not known [16], but it seems evident that the essential part of the decay of this highly excited state in ^{8}Li should result in the appearance of tritons. The ejection angle of triton is restricted to $<30°$ by kinematics, while for protons the corresponding angle is 90°. Taking into account the probabilities and the kinematics, one should expect $\sim 2\times 4 \times 0.86 \approx 7$ more tritons than protons from resonance population of the $T=5/2$ states [2 is the kinematics factor, 4 comes from Eq. (1), and 0.86 is a ratio of neutron to proton decay penetrability factors at the average excitation energy]. The observed ratio of 6.6 is in qualitative agreement with the estimation. A detailed analysis of the decay spectrum in question will be published elsewhere.

The proton spectrum should carry new information on isobaric analog states in ^{9}Li. The 0° proton spectrum is shown in Fig. 3. There are energy limits in both the low- and high-energy parts of this spectrum. At high energies, the proton energy is limited by the available energy of the ^{8}He beam and the ^{8}He+p kinematics. The low-energy cutoff is defined mainly by the energy loss of low-energy protons in the ΔE detector and in the gas. The spectra measured at the two ^{8}He energies agree within 10% (over their common proton energy range). In order to increase the counting statistics, these two spectra were merged at all applicable energies after the transformation to the center-of-momentum system. In the analysis of the proton spectrum, we assumed that only $T=5/2$ resonances dominantly contribute. To begin with, we evaluated the excitation energy of the lowest p state with $T=5/2$ using Eq. (1); the corresponding state in ^{9}He, which is 1.2 MeV above the threshold for ^{8}He+n decay, has been observed in many inclusive spectra from different reactions

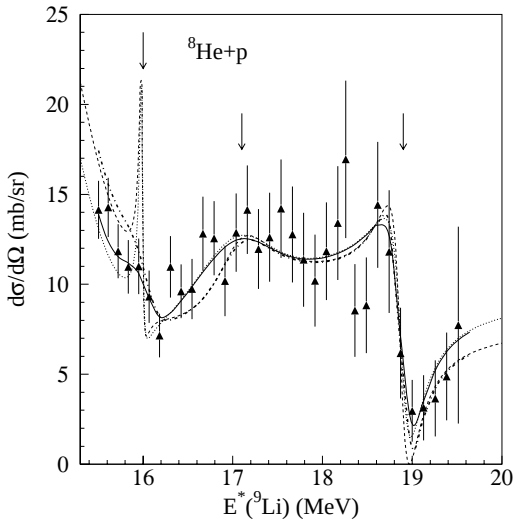

FIG. 3. ^{8}He$+p$ elastic scattering excitation function measured in the 0° telescope. Resonance energies are indicated with arrows (the $3/2^-$ assignment was used for the state at 17.1 MeV).

[1,3,4]. As can be seen from Eq. (1), the ^{8}Li$(T=2)+n$ part gives the main contribution to the energy of the analog state. Therefore, if one assumes the same single particle potential for the interactions of ^{8}Li$(T=2)+n$ and ^{8}He$+n$, the mass defect for the state in question will be

$$\Delta_{^9\mathrm{Li}(T=5/2)} \approx \Delta_{^8\mathrm{Li}(T=2)} + \Delta_n + E_{^9\mathrm{He}}, \tag{2}$$

where $E_{^9\mathrm{He}}$is the energy of the corresponding state in ^{9}He relative to the ^{8}He$+n$ decay threshold. Taking account of the ^{8}He$+p$ channel increases the excitation energy of the $T=5/2$ state by $\sim$50 keV due to the Coulomb interaction. Hence, one should expect the analog state at an excitation energy of about 16.1 MeV in ^{9}Li. The typical precision of this approach is a few hundred keV [15]. We also took into account the results [3,4] on two additional states, at 1.2 MeV and 3.0 MeV above the p-state in ^{9}He, in an R-matrix fit to the experimental data.

The potential scattering (nuclear and Coulomb) was computed with an optical model potential for ^{8}He$+p$ elastic scattering. The parameters for this potential were taken from Ref. [17], in which elastic scattering of ^{8}He$+p$ was consistently fitted over a wide range of energies using the same potential. The real and spin-orbit parts of the potential, as well as the radius and diffuseness of the imaginary part, were held fixed. For the imaginary potential, we used only a surface term as suggested in a recent parametrization of the nucleon optical potential for energies below 10 MeV by Varner *et al.* [18]. The depth of the imaginary part was taken to be energy dependent according to the recommendations of Ref. [19]. The parameters of the potential were as follows: $V_0=39.5$ MeV, $R_0=1.86$ fm, $a_0=0.813$ fm, $V_{s.o.}=1.57$ MeV, $R_{s.o.}=3.58$ fm, $a_{s.o.}=0.459$ fm, $W_s=4.9+0.4\times E$ MeV, $R_s=2.0$ fm, $a_s=0.801$ fm. (R is the total radius and E is the lab. energy of the protons). The resonance positions were varied within 300 keV and the spins and the total widths were considered as free parameters. The ratio of the proton to the neutron reduced width of the resonances was given by isobaric spin conservation [Eq. (1)] and not varied. When a fit to the general features of the excitation function was obtained, we tested the sensitivity of the fit to the presence of an s state, which was found [6] below the p state near the threshold of ^{9}He decay into ^{8}He$+n$ as mentioned above. Unfortunately, the strength of the resonance is not known and its position is only approximately defined [6]. Taking this into account, and considering the importance of the s-wave phase shift for low-energy scattering, we decided to keep the optical model parameters constant and include the parameters of the low-lying s-wave resonance as free parameters. (A few tests of the sensitivity of the results to the optical model parameters were also made.) The specific two-channel expression used for the R-matrix fit is given below. All notations are the same as in Ref. [20],

$$U_{cc}^{J\ell} = U_{cc}^{J\ell}pot + \exp[2i(\omega_\ell + \delta_{J\ell})]2iP_\ell[R_{11}^{J\ell} - L_2^\ell(R_{11}^{J\ell}R_{22}^{J\ell} - R_{12}^{J\ell 2})]d^{-1}, \tag{3}$$

$$d = (1-R_{11}^{J\ell}L_1^\ell)(1-R_{22}^{J\ell}L_2^\ell) - L_1^\ell R_{12}^{J\ell 2} L_2^\ell,$$

$$U_{cc}^{J\ell}pot = \exp[2i(\omega_\ell + \delta_{J\ell})], \tag{4}$$

$$R_{mk}^{J\ell} = \sum_\lambda \gamma_{m\lambda}^{J\ell}\gamma_{k\lambda}^{J\ell}/(E_\lambda - E), \tag{5}$$

$$\delta_{J\ell} = \lambda + i\mu. \tag{6}$$

Here, δ is a complex phase obtained from the optical model calculations.

The results of the fit are summarized in Table I. The R-matrix calculation assuming $1/2^-$ spin for the first resonance, $3/2^-$ for the second, and $5/2^+$ for the third is shown in Fig. 3 by a dashed line. The convolution of this calculation with the experimental resolution function is shown by the bold dot-dashed line. The experimental resolution function

TABLE I. Parameters of $T=5/2$ resonances in ^{9}Li obtained from the R-matrix fit, compared with ^{9}He resonances from Refs. [1,4].

I^π	$E^*(^9\mathrm{Li})$	Γ_t (keV)	$E^*(^9\mathrm{He})$ [a]	$E^*(^9\mathrm{He})$ [1]	$E^*(^9\mathrm{He})$ [4]	$\Gamma_t(^9\mathrm{He})$ (keV) [4]
$1/2^-$ $(3/2^-)$	16.0 ± 0.1	<100	1.1	1.13 ± 0.1	1.27 ± 0.1	100 ± 60
$3/2^-$ $(1/2^-;1/2^+)$	17.1 ± 0.2	800 ± 300	2.2	2.3	2.4 ± 0.1	700 ± 200
	(17.3 ± 0.25) [b]	(1100 ± 400) [b]				
$5/2^+$ $(3/2^+)$	18.9 ± 0.1	240 ± 100	4.0		4.3 ± 0.1	Narrow

[a]Resonance energies in ^{9}He were estimated using Eq. (2). Energy is given relative to the ^{8}He$+n$ decay threshold.
[b]Values in parentheses are for the $1/2^+$ assignment.

was generated by a Monte Carlo code that took into account all the conditions of the experiment. The effective energy resolution near the third resonance (18.9 MeV) is about 100 keV. This deteriorates with decrease of the excitation energy, reaching about 400 keV near the first resonance (16.0 MeV). Equivalent fits were obtained with spin $3/2^-$ for the 16.0 MeV state and spin $1/2^-$ for the 17.1 MeV resonance. This results from the fact that the resonance profile is mainly dependent upon the orbital angular momentum. For the broad 17.1 MeV resonance, a $1/2^+$ assignment is also possible and even gives a somewhat better fit to the data as can be seen in Fig. 3 (solid bold curve for the convoluted fit; dotted curve for the unconvoluted fit). However, the corresponding state in ^{9}He was observed in massive transfer reactions [3,4] with rather high probability, while well known *s*-wave states in ^{11}Be and in ^{11}N were not observed (see Refs. [4,22]). Also, our analysis for an *s*-wave state (see Table I) gives somewhat different values for the position and the width of this resonance in comparison with the data of Refs. [3,4]. These facts might be considered as an indication against a $1/2^+$ assignment for the resonance in question.

As can be seen in Fig. 3, a good fit to the experimental data can be achieved without the *s*-wave resonance [6] in the low-energy region. A broad *s*-wave state introduced into the low-energy region deteriorates the fit, and it cannot be improved by variations of the parameters of the other resonances. The *s*-wave resonance can be positioned rather far from the investigated region, at 14.3 MeV (or lower), if its reduced width is less than 0.1 times the single particle width. This resonance position agrees with the data of Ref. [6]. The strength of the resonance is not known. However, recent calculations [23] showed that the s^2 component for the last two neutrons in the ground state of the $A=8, T=2$ nucleus is negligible. Therefore a large reduced width could be expected for an *s*-wave resonance in ^{9}He. Also, it is worthwhile to mention that the intruder *s*-wave state in ^{8}B [10,12] and ^{11}N [9,11] manifests itself as a very broad resonance. We checked the possibility to include such a broad *s*-wave resonance in the low-energy region by changing the nuclear potential scattering. A decrease of the imaginary part of the optical-model potential will result in an increase of the cross sections for the potential scattering (and therefore the *R* matrix cross sections). In this case, inclusion of the broad *s*-wave state would improve the fit due to destructive interference in the measured energy range, while the above conclusions on the parameters of higher resonances would still be valid. Taking into account the uncertainties of the optical-model potential for the low-energy $p+^8$He scattering, the presence of the broad *s*-wave state—the analog of the hypothetical ground state in ^{9}He [6]—cannot be excluded by the present measurements.

In summary, we found three resonances at excitation energies of 16.0; 17.1 (17.3), and 18.9 MeV in ^{9}Li, which we believe are $T=5/2$ states, the isobaric analogs of states in ^{9}He. The relative positions of the states and their widths are in agreement with data [3,4] on ^{9}He states (see Table I) and their neutron to proton partial width ratios correspond to Eq. (1). We also gave restrictions on the spin assignments of the resonances.

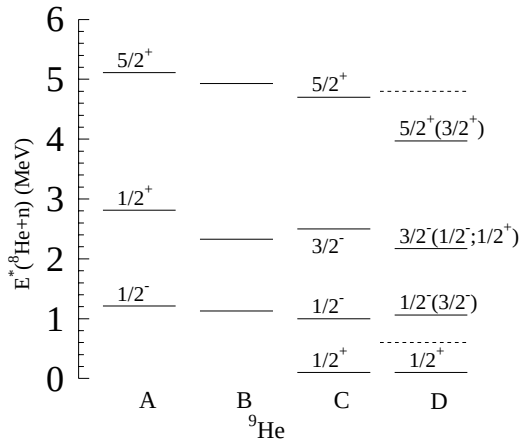

FIG. 4. Spectroscopy of low lying states in ^{9}He. (a) Shell-model predictions from Ref. [2]. (b) Experimental result from Ref. [1]. (c) Modern shell-model calculations [6] with the WBT interaction of Warburton and Brown [21], shifted by 4.0 MeV (in this calculation ^{9}He appeared to be unbound by 4.1 MeV). (d) Levels observed in this work, with the additional $1/2^+$ level from Ref. [6]. Dashed lines correspond to the energy window of this experiment. Equation (2) was used to calculate excitation energies of ^{9}He levels from the observed ^{9}Li($T=5/2$) resonances.

Figure 4 presents different theoretical predictions for the lowest states in ^{9}He, together with the experimental results. Figure 4(a) presents the calculation of Ref. [2], which was used in the first experimental work on ^{9}He [1]. Figure 4(b) gives the experimental level scheme of Ref. [1]; the tentative spin assignments were assumed to correspond to the predictions of Ref. [2]. Figure 4(c) gives the latest calculation [6], and Fig. 4(d) the experimental results of this work, with the addition of a possible *s*-wave state found in Ref. [6]. As can be seen from Fig. 4, the present results without the lowest *s*-wave state could be put into agreement with the older calculations. The lowest (ground) state of ^{9}He would be $1/2^-$ in this case. However, the narrow width of this state, which corresponds to about 1/10 of the single particle width, contradicts the assumed dominant neutron structure of ^{9}He as $(p3/2)^4(p1/2)^1$. Comparing with the latest predictions, the narrow width of the $p1/2$ state is also surprising, especially considering the broad $3/2^-$ state. The above considerations give evidence that the ^{9}He nucleus, with its very unusual neutron to proton ratio, really has an unusual structure.

Some additional measurements could be very important to fix the spin assignments for levels in ^{9}He (or for $T=5/2$ levels in ^{9}Li). The lower part of the excitation function, which could not be measured in the present experiment, should give information on potential scattering and on the existence of the low-energy *s*-wave state. It is not possible to improve the present data by using a magnetically separated beam. To move further, it is necessary to decrease the energy of the ^{8}He beam and to improve its energy resolution, but this will result in a drop in the beam intensity. Better results can be obtained with an Isolde-type beam. With better low-energy data, the parameters of the resonances at higher energy could be obtained with much better precision. Also, the measurement of the neutron decay of the states in question would be very informative. The resonance cross section

should be several times larger, and the data would be free from the confusing potential scattering.

The authors are indebted to Professor E. Saperstein and Dr. L. Grigorenko for fruitful discussions, to Professor M.G. Itkis for support of this work, and to Professor Becchetti for providing silicon detectors for these measurements. This work was supported by NSF Grant No. PHY99-01133, DoE Grant No. DE-FG03-93ER40773, and RFBR Grant No. 02-02-16550.

[1] K.K. Seth, M. Artuso, D. Barlow, S. Iversen, M. Kaletka, H. Nann, and B. Parker, Phys. Rev. Lett. **58**, 1930 (1987).
[2] N.A.F.M. Poppelier, L.D. Wood, and P.W.M. Glaudemans, Phys. Lett. **157B**, 120 (1985).
[3] W. von Oertzen *et al.*, Nucl. Phys. **A588**, 129c (1995).
[4] H.G. Bohlen, A. Blazevic, B. Gebauer, W. von Oertzen, S. Thummerer, R. Kalpakchieva, S.M. Grimes, and T.N. Massey, Prog. Part. Nucl. Phys. **42**, 17 (1999).
[5] Yu.E. Penionzhkevich, Hyperfine Interact. **132**, 265 (2001).
[6] L. Chen, B. Blank, B.A. Brown, M. Chartier, A. Galonsky, P.G. Hansen, and M. Thoennessen, Phys. Lett. B **505**, 21 (2001).
[7] T. Otsuka, R. Fujimoto, Y. Utsuno, B.A. Brown, M. Honma, and T. Mizusaki, Phys. Rev. Lett. **87**, 082502 (2001).
[8] S. Aoyama, Phys. Rev. Lett. **89**, 052501 (2002).
[9] L. Axelsson *et al.*, Phys. Rev. C **54**, R1511 (1996).
[10] V.Z. Goldberg, G.V. Rogachev, M.S. Golovkov, V.I. Dukhanov, I.N. Serikov, and V. Timofeev, JETP Lett. **67**, 1013 (1998).
[11] K. Markenroth *et al.*, Phys. Rev. C **62**, 034308 (2000).
[12] G.V. Rogachev *et al.*, Phys. Rev. C **64**, 061601 (2001).
[13] V.Z. Goldberg, in *ENAM98, Exotic Nuclei and Atomic Masses*, edited by Bradley M. Sherrill, David J. Morrisey, and Cary N. Davids, AIP Conf. Proc. No. 455 (AIP, Woodbury, NY, 1998), p. 319.
[14] A. Rodin *et al.*, Nucl. Instrum. Methods Phys. Res. B **126**, 236 (1996).
[15] A. Bohr and B. R. Mottelson, *Nuclear Structure* (Benjamin, New York, 1969).
[16] F. Ajzenberg-Selove, Nucl. Phys. **A490**, 1 (1988).
[17] D. Gupta, C. Samanta, and R. Kanungo, Nucl. Phys. **A674**, 77 (2000).
[18] R.L. Varner, W.J. Thompson, T.L. McAbee, E.J. Ludwig, and T.B. Clegg, Phys. Rep. **201**, 57 (1991).
[19] J. Rapaport, Phys. Rep. **87**, 25 (1982).
[20] A.M. Lane and R.G. Thomas, Rev. Mod. Phys. **30**, 257 (1958).
[21] E.K. Warburton and B.A. Brown, Phys. Rev. C **46**, 923 (1992).
[22] A. Lepine-Szily *et al.*, Phys. Rev. Lett. **80**, 1601 (1998).
[23] H.T. Fortune and R. Sherr, Phys. Rev. C **66**, 017301 (2002).